2011

Synthesis, characterization, DNA interaction and cleavage, and in vitro cytotoxicity of copper(II) mixed-ligand complexes with 2-phenyl-3-hydroxy-4(1H)-quinolinone

Roman Buchtik
Palack´y University

Zdenek Travnicek
Palack´y University

Jan Vanco
Palack´y University

Radovan Herchel
Palack´y University

Zdenek Dvorak
Palack´y University

Dalton Transactions

Cite this: *Dalton Trans.*, 2011, **40**, 9404

www.rsc.org/dalton

PAPER

Synthesis, characterization, DNA interaction and cleavage, and *in vitro* cytotoxicity of copper(II) mixed-ligand complexes with 2-phenyl-3-hydroxy-4(1*H*)-quinolinone†

Roman Buchtík,[a] Zdeněk Trávníček,*[b] Ján Vančo,[b] Radovan Herchel[a] and Zdeněk Dvořák[c]

Received 15th April 2011, Accepted 5th July 2011
DOI: 10.1039/c1dt10674k

A series of mixed-ligand complexes $[Cu(qui)(L)]NO_3 \cdot xH_2O$ (**1–6**), where Hqui = 2-phenyl-3-hydroxy-4(1*H*)-quinolinone, L = 2,2′-bipyridine (bpy) (**1**), 1,10-phenanthroline (phen) (**2**), bis(2-pyridyl)amine (ambpy) (**3**), 5-methyl-1,10-phenanthroline (mphen) (**4**), 5-nitro-1,10-phenanthroline (nphen) (**5**) and bathophenanthroline (bphen) (**6**), have been synthesized and fully characterized. The X-ray structures of $[Cu(qui)(phen)]NO_3 \cdot H_2O$ (**2**) and $[Cu(qui)(ambpy)]NO_3$ (**3a**) show a slightly distorted square-planar geometry in the vicinity of the central copper(II) atom. An *in vitro* cytotoxicity study of the complexes found significant activity against human osteosarcoma (HOS) and human breast adenocarcinoma (MCF7) cell lines, with the best results for complex **6**, where IC_{50} equals to 2.1 ± 0.2 μM, and 2.2 ± 0.4 μM, respectively. The strong interactions of the complexes with calf thymus DNA (CT-DNA) and high ability to cleave pUC19 DNA plasmid were found. A correlation has been found between the *in vitro* cytotoxicity and DNA cleavage studies of the complexes.

Introduction

The medicinal importance of cisplatin and other platinum-based drugs[1,2] has resulted in an extensive search for a broad spectrum of transition metal-based complexes that could be used in the treatment of malignant tumours. Due to the generally high toxicity and unwanted side-effects of platinum-based complexes, we have focused our attention on the more favourable transition metal for biological systems, *i.e.* copper. Copper is one of the metals acting as an essential trace element involved in cellular respiration, antioxidant defence, neurotransmission, connective tissue biosynthesis and cellular iron metabolism. Several investigations provide evidence that copper ions are capable of interacting directly with nuclear proteins and DNA, causing site-specific damage.[3,4] It has been reported that copper compounds delay cell-cycle progression and increase cell death in different cell cultures.[5,6] Copper(II) ions binding to specific sites can modify conformational structures of proteins, polynucleotides, DNA or membranes. Cu(II) binds to DNA with high affinity and thus promotes DNA oxidation.[7] It also causes apoptosis in cultured mammalian cells.[8]

Back in 1965, Dwyer and co-workers first reported that a Cu(II) complex of the composition of $[Cu(tmphen)_2]Cl_2$, where tmphen stands for 3,4,7,8-tetramethyl-1,10-phenanthroline, inhibits the growth of Landschütz ascites tumour.[9] Since then, anticancer properties of a wide range of copper complexes containing 1,10-phenanthroline (phen) and related ligands have been intensively investigated.[10–13] However, the mechanism by which these complexes enforce their biological activity is still unknown. It can be supposed that the complexes bind directly to target molecules within the cell or they participate in the redox system that produces radicals consecutively damaging the molecules within the cell. The next generation of the above-mentioned complexes is represented by Casiopeínas, a group of Cu(II) mixed-ligand antineoplastic agents, containing 1,10-phenanthroline (phen), 2,2′-bipyridine (bpy) derivatives in combination with essential aminoacids.[14–16] These compounds exhibit cytotoxicity, genotoxicity and antitumour effects, however, the mechanism of their action has also not been determined yet.

We have several reasons for choosing 2-phenyl-3-hydroxy-4(1*H*)-quinolinone (Fig. 1) as the crucial ligand for the preparation of the complexes (**1–6**). Firstly, generally 4-quinolinones, as aza-analogues of flavones, are well known for their wide range of diverse biological activities, such as antibacterial activity due to the inhibition of DNA-gyrase (a class of enzymes known as topoisomerases) or antitumour activity, which is presumably caused by mammalian topoisomerase II inhibition.[17–19] Secondly the advantage of a study of 2-phenyl-3-hydroxy-4(1*H*)-quinolinone

[a]*Department of Inorganic Chemistry, Faculty of Science, Palacký University, 17. listopadu 12, CZ-771 46, Olomouc, Czech Republic*
[b]*Regional Centre of Advanced Technologies and Materials, Department of Inorganic Chemistry, Faculty of Science, Palacký University, 17. listopadu 12, CZ-771 46, Olomouc, Czech Republic. E-mail: zdenek.travnicek@upol.cz; Fax: +420585 634 954; Tel: +420 585 634 352*
[c]*Regional Centre of Advanced Technologies and Materials, Department of Cell Biology and Genetics, Faculty of Science, Palacký University, Šlechtitelů 11, CZ-783 71, Olomouc, Czech Republic*

† Electronic supplementary information (ESI) available. CCDC reference numbers 822513–822515. For ESI and crystallographic data in CIF or other electronic format see DOI: 10.1039/c1dt10674k

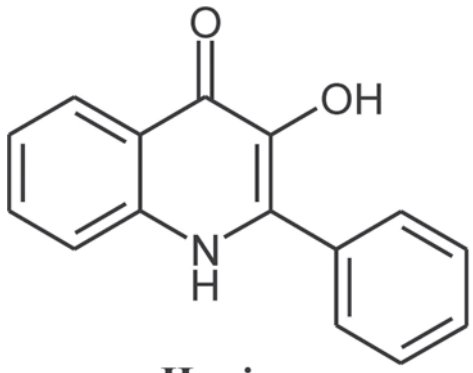

Hqui

Fig. 1 A representation of 2-phenyl-3-hydroxy-4(1*H*)-quinolinone (Hqui), which was used as a ligand for the preparation of complexes **1–6**.

complexes of suitable transition metals is the fact that 2-phenyl-3-hydroxy-4(1*H*)-quinolinones themselves, as a specific group of 4-quinolones, have already been studied for their potential biological activity only recently due to their long time synthetic unavailability.[20] Finally complexes involving these ligands are practically unknown, except for $[Cu(qui)_2]$ and [Cu(tmeda)(qui)(*N*-baa)] complexes, where tmeda and N-baa stand for *N*,*N*,*N*′,*N*′-tetramethyl-ethane-1,2-diamine, and 2-(benzoylamino)benzoate, respectively.[21]

During this work, we strived not only to prepare and characterize a novel group of copper(II) complexes and to broaden a spectrum of Casiopeínas-like complexes but also to find out if the prepared complexes show *in vitro* cytotoxicity against selected human cancer cell lines. Thus, we focused on studying Cu(II) mixed-ligand complexes of the general composition $[Cu(qui)(L)]NO_3 \cdot xH_2O$, where qui = 2-phenyl-3-hydroxy-4(1*H*)-quinolinonate anion and L = 2,2′-bipyridine (bpy), 1,10-phenanthroline (phen), 2,2′-bipyridylamine (ambpy), 5-methyl-1,10-phenanthroline (mphen), 5-nitro-1,10-phenanthroline (nphen) or bathophenanthroline (bphen).

Experimental

Complexes of the composition $[Cu(qui)(bpy)]NO_3 \cdot 1/2H_2O$ (**1**), $[Cu(qui)(phen)]NO_3 \cdot H_2O$ (**2**), $[Cu(qui)(ambpy)]NO_3 \cdot 1/2H_2O$ (**3**), $[Cu(qui)(mphen)]NO_3 \cdot H_2O$ (**4**), $[Cu(qui)(nphen)]NO_3 \cdot H_2O$ (**5**) and $[Cu(qui)(bphen)]NO_3 \cdot H_2O$ (**6**), have been synthesized *via* the reaction of 2-phenyl-3-hydroxy-4(1*H*)-quinolinone (Hqui) and the corresponding bidentate N-donor ligand (L) with copper(II) nitrate in an ethanol/water mixture (11 : 1, v/v) in the 1 : 1 : 1 molar ratios, with average yields of 55–67%. They were characterized by elemental analysis, UV-Vis, FTIR, Raman and EPR spectroscopy, mass spectrometry, magnetic, conductivity and thermogravimetric TG/DTA measurements, and single crystal X-ray analysis (for detailed methodology used and the syntheses see ESI S1, S2†).

Cytotoxicity *in vitro*

Human cancer cell lines were purchased from a European Collection of Cell Cultures (ECACC). Human Caucasian osteosarcoma cells (HOS; ECACC No.87070202) and human Caucasian breast adenocarcinoma cells (MCF7; ECACC No.86012803) were used in the study. Cells were cultured according to the manufacturer's instructions. Cells were maintained at 37 °C and 5% CO_2 in a humidified incubator.

Human cancer cell lines were treated with the tested compounds for 24 h and 48 h, using 96-well culture plates.[22] The tested compounds (cisplatin and **1–6**) were applied to the cells at concentrations of 0.1, 1, 10, 25 and 50 μM. In parallel, the cells were treated with vehicle (DMF; 0.1% v/v) and Triton X-100 (1% v/v) to assess the minimal (*i.e.* positive control) and maximal (*i.e.* negative control) cell damage, respectively. The MTT assay [MTT = 3-(4,5-dimethylthiazol-2-yl)-2,5-diphenyltetrazolium bromide] was measured at TECAN, Schoeller Instruments LLC (540 nm). The data were expressed as the percentage of viability, when 100% and 0% represent the treatments with DMF and Triton X-100, respectively. The data from cancer cell lines were acquired from three independent cell passages. The values of IC_{50} were calculated, unless the concentration of the tested compound was limited by its solubility.

DNA interactions assessed by UV-Vis titration

The UV-Vis titration experiments were performed as a supplemental method for analyzing the efficiency and prediction of the possible mechanism of complex-DNA interaction. The method is based on measuring the absorption spectra of mixtures, containing the same concentration of the tested complexes at 50 μM and varying concentrations of the nucleic acid. All experiments involving the interactions of the tested compounds with CT-DNA were performed in Tris/HCl buffer [tris(hydroxymethyl)aminomethane], containing 5 mM Tris and 50 mM NaCl, adjusted to pH 7.2 by the addition of HCl. The DNA samples were prepared by the dilution of viscous saturated solutions of CT-DNA in Tris/HCl buffer (approx. conc. 4 mg mL^{-1}), which spectral analysis at 260 nm and 280 nm gave the ratios of *ca* 1.8–1.9, indicating that CT-DNA was sufficiently free of protein.[23] The absorption spectra were analyzed for the nucleic acid concentration-dependent changes, like bathochromic (red-shift), hypsochromic (blue-shift), or hypochromic effects, usually considered as the evidence of DNA interactions.[24]

DNA cleavage studies

Supercoiled plasmid DNA pUC19 was obtained by the standard isolation process from *Escherichia coli* TOP10F cells using the preparation kit QIAprep Spin Miniprep Kit (Qiagen, Hilden, Germany), and its purity was checked by UV-Vis spectroscopy at 230, 260, 280, and 320 nm. The native pUC19 plasmid was solubilized in TE buffer (10 mM Tris, 1 mM EDTA, pH = 8.0, final concentration 23.1 μM calculated as base-pairs). Supercoiled plasmid (3–5 μL per reaction) was mixed with various concentrations of the tested complexes (in different experiments, various final concentrations of the Cu(II) complex to one base pair (bp) of dsDNA were used, usually 1 : 1, 5 : 1, and 10 : 1 bp) in the presence and absence of the reducing agent L-ascorbic acid in TE buffer. Reaction mixtures were incubated at 37 °C for 1 h and then analyzed by 0.8% agarose gel electrophoresis and detected with ethidium bromide staining. The electrophoreogram was analyzed by the software AlphaEaseFC version 4.0.0.34 (Alpha Innotech, USA) and the relative percentages of the supercoiled circular

(CCC) form, single-strand nicked (OC) form and linear (L) form were evaluated.

Cytological visualization of copper

The cytological visualization experiment was performed on a culture of human acute monocyte leukemia cells (THP-1, ATCC). The THP-1 cells were cultured (in RPMI-1640 supplemented with 10% FBS and 1% of mixture of penicillin and streptomycin) for 24 h with a 5 μM DMSO solution of Cu(II) complex and the control sample was cultivated with dimethylsulfoxide as vehicle. The culture medium over the adherent THP-1 cells was removed from the culture dish and the cells were washed with 6.7 mM phosphate buffer solution (pH = 7.4). The cells were fixed for 30 min by a 70% ethanol solution at 4 °C. After fixation, 500 μl of rhodanine working solution, prepared by adding 1 ml of saturated ethanolic solution of 5-(dimethylamino)benzylidenerhodanine (Sigma-Aldrich) to 30 ml of distilled water, was pipetted into each culture dish. The culture dishes were incubated for 2 h at 60 °C and then the changes in colour were evaluated by light microscopy at 120× magnification.

Interaction with human serum albumin

Deconvolution analysis of ESI-MS spectra of mixtures of Cu(II) complex **2** (at 40 and 400 μM concentrations) with HSA (human serum albumin, Sigma-Aldrich, at 40 μM) were carried out. The HSA and complex **2** were both separately diluted in 2.5 mM ammonium acetate dissolved in 2% acetic acid. The mass spectra of the interacting systems were measured for a period of 30 min starting with the addition of the corresponding complex to the HSA solution, and the last spectra (in the 30th minute) were evaluated by deconvolution analysis using the Promass for Xcalibur, ver. 2.8, the automated ESI-deconvolution software (Novatia LLC).

Results and discussion

Characterization

The colour of the prepared crystalline products varied from yellow-green (**1–4**), through greenish brown (**5**) to dark brown (**6**). The compounds, excluding complex **5**, have been found to be very soluble in DMF and DMSO, while their solubility in ethanol, acetone and water is very low. The solubility of complex **5** is low even in DMF and DMSO, presumably due to the substitution on 1,10-phenanthroline, which increases its hydrophobic character and makes the metal complexes soluble in a limited range extent (up to 10^{-3} M), and moreover, the solubility of the complex in water was even lower. Each of the complexes behaved as an electrolyte 1 : 1 in DMF solutions, which corresponds to the presumption of dissociation of the complexes in the solvent used into the $[Cu(qui)(L)]^+$ cation and nitrate anion. ESI-MS spectra provided direct evidence about the formation of the $[Cu(qui)(L)]^+$ complex cations, whose peaks have been observed. The MS^2 spectra of the complexes afforded the same fragmentation, the loss of the 2-phenyl-3-hydroxy-4(1*H*)-quinolinonate anion was observed in all the cases with the $[Cu(L)]^+$ peak as the product of the fragmentation. The MS^2 spectrum of complex **2**, as a representative example, is shown in ESI (Fig. S3†).

TG curves confirmed the presence of the water molecules of crystallization in the complexes, the compounds **1** and **3** have been determined as hemihydrates, while complexes **2** and **4–6** are monohydrates. The thermal decomposition data are listed above in preparation of complexes section, TG/DTA curves of **1–6** are shown in ESI (Fig. S4†). The determined weight losses correlated well with those calculated for the final product (CuO).

X-ray structure of $[Cu(qui)(phen)]NO_3 \cdot H_2O$ (2) and $[Cu(qui)(ambpy)]NO_3$ (3a)

The molecular structures of **2** and **3a** were determined and are shown in Fig. 2, and Fig. 3, respectively. The crystal data and structure refinements are given in Table 1, the selected bond lengths and angles are listed in Table 2. The geometry of the CuN_2O_2 chromophore in both the complexes is distorted square-planar. The Cu1–N2 and Cu1–N3, and Cu1–O1 and Cu1–O2 bond lengths of **2** and **3a** (see Table 2) correlate well with the mean value of 1.981 Å (1.947–2.107 Å interval; for Cu–N) and 1.923 Å (1.869–2.182 Å interval; Cu–O) determined for both discussed bond types for eighteen Cu(II) complexes involving the square-planar N_2O_2 donor set deposited in the Cambridge Structural Database CSD to date.[25] A degree of deformation in the vicinity of the central Cu(II) atoms can be also seen from the deviations from the least-square planes fitted through the CuN_2O_2 atoms, which were found to be (in Å): Cu1 = –0.0008(3), O1 = –0.0185(2), O2 = 0.0297(2), N1 = –0.0409(2) and for N2 = 0.0613(2) for complex **2**; Cu1 = 0.0033 (3), O1 = –0.117 (3), O2 = –0.004 (3), N2 = –0.014 (3) and for N3 = –0.116 (3) for complex **3a**.

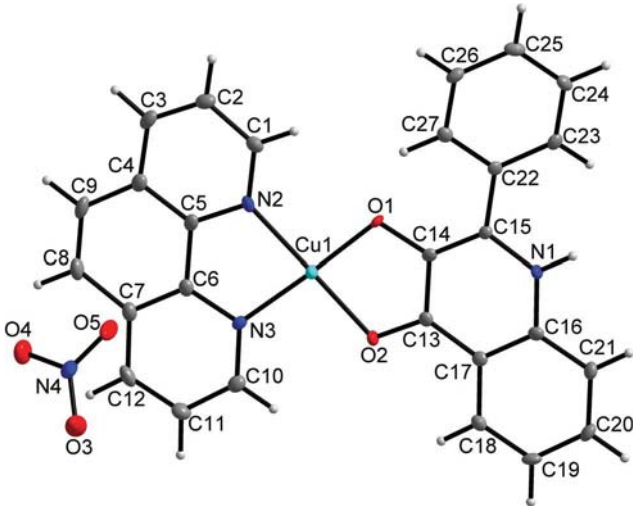

Fig. 2 Molecular structure of complex **2** together with the atom numbering scheme. The water molecule of crystallization was omitted for clarity. The non-H atoms are drawn as thermal ellipsoids at the 50% probability level.

The two bidentate chelating ligands qui (excluding the phenyl group of qui) and L are almost coplanar with the dihedral angle being 2.65(4)° (for **2**) and 3.34(6)° (for **3a**). The dihedral angle between the phenyl ring and a quinoline moiety in qui was found to be 26.72(5)° (for **2**) and 36.38(8)° (for **3a**).

In the crystal structure of **2**, the isolated $[Cu(qui)(phen)]^+$ cations, nitrate anions and crystal water molecules are held together *via* the N–H···O and O–H···O hydrogen bonds and

Table 1 Crystal data and structure refinements for $[Cu(qui)(phen)]NO_3 \cdot H_2O$ (**2**) and $[Cu(qui)(ambpy)]NO_3$ (**3a**)

Compound	**2**	**3a**
Empirical formula	$C_{27}H_{20}CuN_4O_6$	$C_{25}H_{19}CuN_5O_5$
Formula weight	560.02	532.99
T/K	100(2)	100(2)
Crystal system, space group	Monoclinic, $P2_1/n$	Monoclinic, Cc
Unit cell dimensions		
a/Å	17.5992(5)	14.0853(7)
b/Å	7.1785(2)	22.5202(11)
c/Å	19.0423(5)	6.8273(4)
α (°)	90	90
β (°)	111.443(3)	95.373(5)
γ (°)	90	90
V/Å^3	2239.19(10)	2156.1(2)
Z, D_c/g cm^{-3}	2, 1.660	4, 1.642
Absorption coefficient (mm^{-1})	1.032	1.065
Crystal size/mm	0.35 × 0.10 × 0.10	0.20 × 0.10 × 0.10
F(000)	1146	1092
θ range for data collection (°)	$3.06 \le \theta \le 25.00$	$2.91 \le \theta \le 25.00$
Index ranges (h, k, l)	$-20 \le h \le 20$ $-8 \le k \le 8$ $-22 \le l \le 22$	$-13 \le h \le 16$ $-26 \le k \le 26$ $-8 \le l \le 8$
Reflections collected/unique (R_{int})	18461/3939(0.0450)	9658/3083 (0.0302)
Max. and min. transmission	0.9038 and 0.7140	0.9010 and 0.8152
Data/restraints/parameters	3939/2/346	3083/2/325
Goodness–of–fit on F^2	0.952	1.042
Final R indices [$I > 2\sigma(I)$]	$R_1 = 0.0331$, w$R_2 = 0.0793$	$R_1 = 0.0296$, w$R_2 = 0.0750$
R indices (all data)	$R_1 = 0.0503$, w$R_2 = 0.0826$	$R_1 = 0.0316$, w$R_2 = 0.0759$
Largest peak and hole/e Å^{-3}	0.539, –0.307	0.675, –0.470

Table 2 Selected bond lengths (Å) and angles (°) for $[Cu(qui)(phen)]NO_3 \cdot H_2O$ (**2**) and $[Cu(qui)(ambpy)]NO_3$ (**3a**)

Bond Lengths	**2**	**3a**	Bond Angles	**2**	**3a**
Cu1–O1	1.892(2)	1.918(2)	O2–Cu1–N2	177.87(8)	173.90(11)
Cu1–O2	1.916(2)	1.956(2)	O1–Cu1–N3	176.22(8)	172.26(11)
Cu1–N2	1.978(2)	1.995(3)	O1–Cu1–O2	86.81(7)	83.70(10)
Cu1–N3	1.988(2)	1.988(3)	N3–Cu1–N2	82.92(9)	93.03(12)
N2–C1	1.334(3)	1.360(5)	O2–Cu1–N3	95.84(7)	92.97(10)
N2–C5	1.356(3)	1.350(5)	O1–Cu1–N2	94.51(7)	90.20(12)
N3–C10	1.334(3)	1.353(4)	C1–N2–Cu1	128.82(17)	116.9(2)
N3–C6	1.366(3)	1.351(4)	C5–N2–Cu1	112.68(15)	124.5(3)
N1–C15	1.372(3)	1.354(5)	C10–N3–Cu1	129.73(17)	117.1(2)
N1–C16	1.375(3)	1.373(5)	C6–N3–Cu1	112.10(15)	125.0(2)
O2–C13	1.296(3)	1.312(5)	C13–O2–Cu1	109.55(14)	110.1(2)
O1–C14	1.328(3)	1.317(5)	C14–O1–Cu1	109.79(14)	110.6(2)

C–H···C, C–H···O, N–H···O, C···C and C···O non-covalent contacts (for interatomic parameters of non-covalent contacts see ESI Table S3†). The shortest Cu1···N4 distance between Cu(II) atom and N4 atom of nitrate anion equals 5.791(3) Å. Moreover, the strong intermolecular interactions are present between aromatic rings of phen and qui with the distance of 3.338(2) Å (see Fig. S5†). The O1 atom from qui makes the nearest intermolecular contact to the central copper atom at the distance of 4.38(2) Å.

As for the crystal structure of **3a**, the nitrate anion is situated outside the inner coordination sphere with the shortest Cu1···N5 distance of 6.846(3) Å. The NO_3^- anions are also included in the N–H···O hydrogen bonds towards the N–H groups of ambpy and qui, which results in formation of a one-dimensional polymeric chain. Except of these hydrogen bonds, the crystal structure of **3a** is stabilized by the non-covalent contacts of the C–H···C, C–H···O, N–H···O and C···C type (see ESI Fig. S5†).

UV-Vis, FTIR and Raman spectra

There were three absorption maxima observed in each solid state spectrum in the measured region. The position of the first maximum of all the complexes varies from 404 nm (**1**) to 422 nm (**6**) and due to its very high intensity may be assigned to the charge-transfer (CT) transition. Next two maxima located around 580 and 700 nm may be assigned to the d–d transitions $B_{1g} \rightarrow E_g$ and $B_{1g} \rightarrow B_{2g}$ in quasi D_{4h} point group symmetry of square planar chromophore (Table 3).[26] The electronic spectra were also measured in DMF solutions, in which the CT transition was observed in similar region close to 400 nm. On the contrary, the pattern of the d–d transitions was significantly altered and the only one absorption maximum was observed in the range of 590–620 nm (ε_{max} ranging from 51 to 154 mol^{-1} dm^3 cm^{-1}), which might be explained by the coordination of the solvent to the metal centre resulting in the changing of configuration from square-planar to

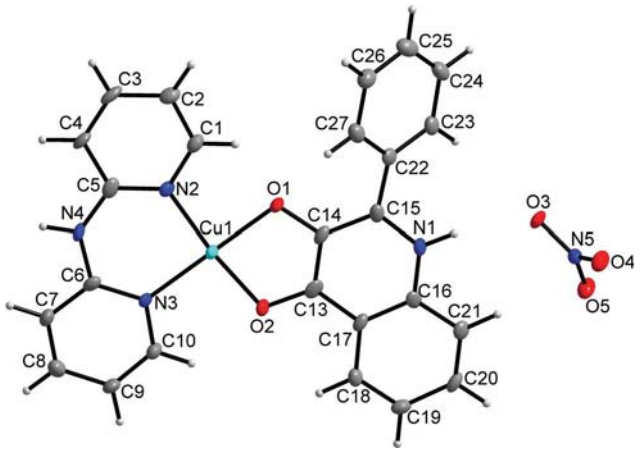

Fig. 3 Molecular structure of complex **3a** together with the atom numbering scheme. The non-H atoms are drawn as thermal ellipsoids at the 50% probability level.

Table 3 Electronic solid state and 10^{-3} DMF solution spectral data for complexes **1–6**

	Solid (CT)	Solid (*d–d*)		DMF (10^{-3} M)	
	λ (nm)	λ_1 (nm)	λ_2 (nm)	λ (nm)	ε (mol^{-1} dm^3 cm^{-1})
1	404	583	692	601	84
2	416	584	707	608	85
3	405	595	760	607	51
4	413	514	709	615	82
5	415	603	709	620	83
6	422	588	706	590	154

Table 4 Selected FTIR spectral data (cm^{-1}) for complexes **1–6**

	Nujol (150–600 cm^{-1})		KBr (400–4000 cm^{-1})		
	ν(Cu–O)	ν(Cu–N)	$\nu_1(NO_3)$	$\nu(C{=}C_{ar})$	ν(C=O)
1	494	544	1309	1562	1627
2	493	542	1317	1563	1629
3	495	543	1325	1568	1631
4	496	543	1317	1566	1629
5	496	546	1327	1564	1631
6	494	545	1318	1562	1628

a distorted octahedral (see also EPR spectroscopy discussion for more details).

The FTIR spectra measured in the 150–4000 cm^{-1} region indirectly confirmed the coordination of heterocyclic ligands to the Cu(II) atom (Table 4). The characteristic band of the carbonyl groups of the coordinated qui appears at 1628–1631 cm^{-1}, which surprisingly does not differ from those of free Hqui found at 1631 cm^{-1}. The characteristic vibration of $\nu(CC_{ar})$ in the aromatic system present in the uncoordinated bidentate N-donor heterocycles (L) appeared in the range of 1562–1568 cm^{-1}. The bands of a very strong intensity in the region of 1450–1560 cm^{-1} are assignable to the vibrations of $\nu(CC_{ar})$ of qui. The very strong bands of the uncoordinated nitrate group $\nu_1(NO_3)$ were observed in the region of 1309–1327 cm^{-1}. FTIR spectra of the complexes showed new bands in comparison to those of free organic ligands in the region between 150 and 600 cm^{-1}. The very strong bands at 542–546 cm^{-1} might be assigned to ν(Cu–N), (lit.[27] 530–560 cm^{-1}), while other very strong bands at 493–496 could originate in ν(Cu–O), (lit.[27] 500–515 cm^{-1}).

The Raman spectra measured in the 150–3750 cm^{-1} range yielded practically the same information as the spectra measured in FTIR excluding complex **3**, which was not measurable due to its burning in the laser beam.

Table 5 The spin Hamiltonian parameters derived from simulating frozen solution EPR spectra of complexes **1–6** in DMF measured at liquid nitrogen temperature

	g_{xy}	g_z	A_{xy} (MHz)	A_z (MHz)
1	2.05	2.24	38	569
2	2.06	2.25	30	551
3	2.06	2.25	31	549
4	2.06	2.26	32	560
5	2.06	2.26	30	562
6	2.06	2.26	35	560

Magnetic and EPR data

The X-band EPR spectroscopy was performed at liquid nitrogen temperature both for the powder samples **1–6** as well as for their DMF frozen solutions. Based on the general pattern of the powder spectra and obtained results, the compounds **1–6** can be divided into two groups. As for the first group, the isotropic signals were observed with $g_{eff} = 2.10$; 2.07 and 2.10 for compounds **2**, **3**, and **4**, respectively. The EPR spectrum of **2**, as a representative example, is shown ESI Fig. S8†. The powder spectra of the second group (compounds **1**, **5** and **6**) are more complicated. Three $\Delta M_S = \pm 1$ transitions were observed in the 270–380 mT region accompanied by $\Delta M_S = \pm 2$ transitions around 150 mT (for the sample spectrum of **1** see ESI Fig. S9†). Such transitions indicate the formation of the *quasi-dimers* in the solid state due to the weak intermolecular interactions. On the contrary, the frozen solution spectra in DMF exhibited the same pattern for all the compounds **1–6**. The main features of the experimental spectra were simulated using the EasySpin package including the hyperfine interactions due to nuclear spin of copper $I = 3/2$ with parameters listed in Table 5.[28] The spectrum of **1** is shown in Fig. 4. The *g*-values were found to be 2.05–2.06 and 2.14–2.26 in the perpendicular, and parallel direction, respectively. The hyperfine splitting tensor's components have values of $A_{xy} = 30$–35 and $A_z = 549$–569 MHz. Also, the super-hyperfine splitting was observed corresponding to two nitrogen atoms of the N-donor based ligands L. To conclude, the analysis of the EPR solution spectra comply well with elongated octahedral copper(II) complexes, whose basal plane is formed by $[Cu(qui)(L)]^+$ motif and the axial positions are the most likely occupied by two O-coordinated DMF molecules.[29]

The magnetic measurements were performed on compounds **1** and **2** as representatives of both groups of compounds determined by solid state EPR. The magnetic susceptibility of **1**, calculated from magnetization measured at $B = 1$ T, is monotonously increasing on temperature lowering up to $T_{max} = 3.4$ K and then starts to decrease. This feature is characteristic for antiferromagnetically coupled Cu(II) dimers or one-dimensional polymeric species. Also, the isothermal magnetizations do not resemble the Brillouin function for an isolated paramagnetic monomer with $S = 1/2$ (Fig. 5). Firstly, the susceptibility above $T = 10$ K was successfully fitted to the Curie–Weiss law with $g = 2.14$ and $\Theta = -3.3$ K (see ESI

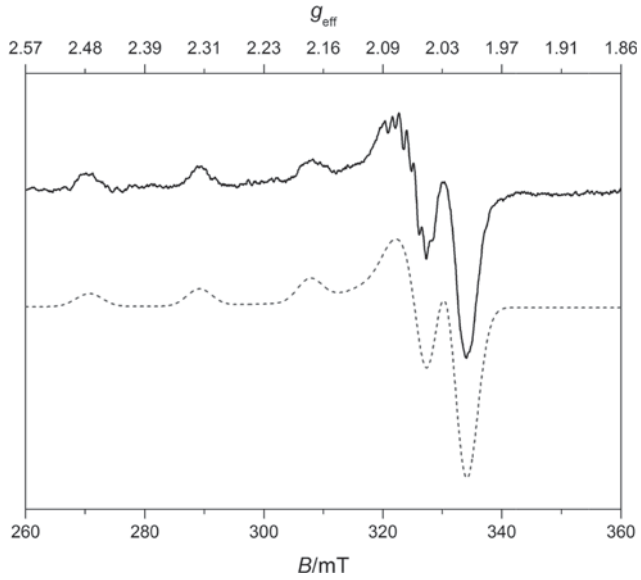

Fig. 4 The frozen solution X-band EPR spectrum of complex **1** in DMF at liquid nitrogen temperature. The experimental data (full line) and calculated data (dashed line) with the parameters given in Table 5.

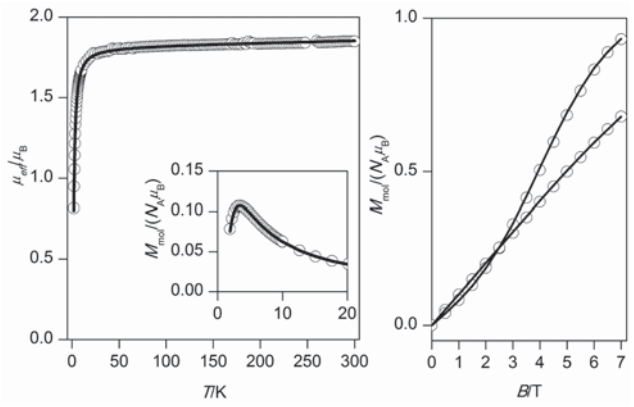

Fig. 5 The magnetic data for complex **1** scaled per one Cu(II). Left: the temperature dependence of the effective magnetic moment and molar magnetization measured at $B = 1$ T. Right: the isothermal magnetizations measured at $T = 2.0$ and 4.6 K. Empty circles – experimental data, full lines – the best fit of experimental data using eqn (1), with $J = -3.9$ cm^{-1} and $g = 2.10$.

Fig. S10†). The negative value of the Weiss constant points out to the presence of antiferromagnetic interactions. Magnetic data for **1** were successfully fitted to the following spin Hamiltonian for dimer

$$\hat{H} = -J(\mathbf{S}_1 \cdot \mathbf{S}_2) + \mu_B \sum_{i=1}^{2} \mathbf{B} \cdot \mathbf{g}_i \cdot \mathbf{S}_i \quad (1)$$

where J-parameter represents the isotropic exchange between two local spins $S_A = S_B = 1/2$. The simple formula for the molar magnetization of such dimer was used

$$M_{mol} = \mu_B g N_A[\exp((J + x)/kT) - \exp((J - x)/kT)]/[1 + \exp((J + x)/kT) + \exp(J/kT) + \exp((J - x)/kT)] \quad (2)$$

where $x = \mu_B gB$ and the fitting procedure resulted in $J = -3.9$ cm^{-1} and $g = 2.10$ (Fig. 4).[30] Such relatively small antiferromagnetic exchange can be understood by forming quasi-dimers in the solid state through the intermolecular interactions as already supported by solid state EPR.

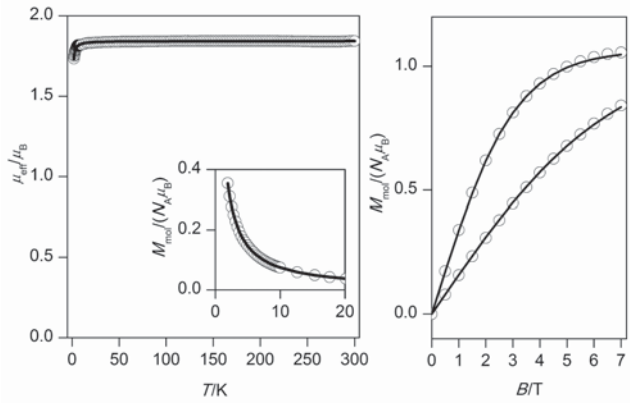

Fig. 6 The magnetic data for complex **2** scaled per one Cu(II). Left: the temperature dependence of the effective magnetic moment and molar magnetization measured at $B = 1$ T. Right: the isothermal magnetizations measured at $T = 2.0$ and 4.6 K. Empty circles – experimental data, full lines – the best fit of experimental data using eqn (3), with $J = -0.23$ cm^{-1} and $g = 2.13$.

The magnetic data of compound **2** are different (Fig. 6). In this case, the molar susceptibility is monotonically increasing on cooling and no maximum is observed. The inverse susceptibility was fitted successfully in the whole temperature range to the Curie–Weiss law with $g = 2.13$ and $\Theta = -0.1$ K (see ESI Fig. S11†). The small and negative value of the Weiss constant is in agreement with decreasing of the effective magnetic moment below 12 K from 1.84 μ_B to 1.72 μ_B at $T = 2$ K. Firstly, we tried to simulate the magnetic behaviour with a monomeric model including molecular field correction zj, but it was unsuccessful. By inspecting the X-ray crystal structure of **2**, we can see forming of the quasi one-dimensional chain through π–π stacking (see ESI Fig. S5†). That is why, the susceptibility was fitted to spin Hamiltonian for antiferromagnetically coupled uniform 1D chain with $S_i = 1/2$ using the Johnston *et al.* equation[31] with $J = -0.30$ cm^{-1} and $g = 2.13$ (see ESI Fig. S12†). In order to fit also the isothermal magnetization data and to confirm our presumption, the magnetic data were fitted to finite-size closed ring model according to spin Hamiltonian

$$\hat{H} = -J\left\{\sum_{i=1}^{16} \mathbf{S}_i \cdot \mathbf{S}_{i+1} + (\mathbf{S}_{17} \cdot \mathbf{S}_1)\right\} + \mu_B \sum_{i=1}^{17} \mathbf{B} \cdot \mathbf{g}_i \cdot \mathbf{S}_i \quad (3)$$

where number of 17 centres is sufficient to mimic infinite chain properties for such small expected antiferromagnetic exchange as was already proved in lit.[32] The fitting procedure resulted in $J = -0.23$ cm^{-1} and $g = 2.13$ (Fig. 6).

In vitro cytotoxicity

All the prepared Cu(II) complexes have been tested for their *in vitro* cytotoxicity against human osteosarcoma (HOS) and human breast adenocarcinoma (MCF7) cancer cell lines. Results are expressed as the IC_{50} values and are summarized in Table 6.

The tested complexes achieved the dose-dependent cytotoxicity in both cancer cell lines. The *in vitro* cytotoxicity of these compounds was in almost all cases considerably higher than

Table 6 *In vitro* cytotoxic activity data together with their standard deviations of complexes **1–6** and cisplatin against the HOS and MCF7 human cell lines, expressed as the IC_{50} values

	HOS[a]	MCF7[b]
1	21.4 ± 5.2	27.2 ± 0.8
2	4.3 ± 0.1	7.3 ± 2.3
3	22.0 ± 5.1	18.9 ± 4.1
4	3.7 ± 0.1	3.9 ± 0.4
5	> 1.0	> 1.0
6	2.1 ± 0.2	2.2 ± 0.4
cisplatin	37.7 ± 5.4	24.5 ± 6.1

[a] human osteosarcoma cell line, [b] human breast adenocarcinoma cell line

those of the commercially used antineoplastic platinum-based drug cisplatin (HOS IC_{50} = 37.7 ± 5.4, MCF7 24.5 ± 6.1 μM) in both human cancer cell lines, and moreover, complex **6** was found to be the most potent one (HOS 2.1 ± 0.2 μM; MCF7 2.2 ± 0.4 μM). The cytotoxicity of compound **5** in all the tested cell types could not be assessed due to its low solubility in an aqueous milieu.

Interaction with CT-DNA assessed by UV-Vis titration

In order to determine a possible mechanism of DNA-copper(II) complex interaction, the spectrophotometric titration of the complexes with highly polymerized CT-DNA was performed. There exist three major modes for binding of metal complexes to DNA: (a) intercalation inside a groove (stabilized by the π–π interactions between the aromatic systems of ligands and nucleobases), (b) binding outside a groove and (c) binding outside the helix (the weakest, mostly electrostatic interaction).[33] Effective intercalation interactions exhibit themselves in UV-Vis spectra through charge-transfer bands by significant hypochromicity and red-shifting of the band maxima (bathochromic effect). The highest hypochromicity was found for complexes **1** and **2** (Table 7, for UV-Vis spectra of the compounds see ESI Fig. S13†), suggesting that these compounds intercalate with DNA more than the others.

On the other hand, the complexes **4** and **5**, involving more hydrophobic ligands 5-methyl-1,10-phenanthroline, and 5-nitro-1,10-phenanthroline, respectively, provided a significantly lower hypochromic effect, which could mean that although these complexes form non-covalent interaction with DNA, the intercalation is just partial, *i.e.* the steric hindrance of their substituents prevent them from penetrating further into the minor groove of DNA and π–π interactions between the aromatic systems of ligands and nucleobases are much less effective. Copper(II) complexes involving low-molecular weight ligands derived from phenanthroline have been identified in many publications as prominent minor-groove binding agents.[34,35] Furthermore, cells undergoing oxidative stress, which is speculated to be the cause or manifestation of more than 100 pathological processes, including some types of cancer and different inflammatory processes, have been shown to undergo oxidative DNA cleavage when exposed to transition metal complexes that bind in the minor groove and are able to participate in the Fenton's reaction.[36–38]

DNA cleavage

DNA cleavage experiments were performed on a model system involving a mixture of circular plasmid pUC19 and the Cu(II) complexes in different concentrations in a state of oxidative stress (*i.e.* Fenton's reaction with hydrogen peroxide either in the presence or absence of a reducing agent, ascorbic acid). The products and intermediates of the reaction (the reactive species CuO^{+} and $Cu(OH)^{2+}$ or the highly reactive hydroxyl radical)[39–41] cause single-strand breaks of the supercoiled double-strand DNA (CCC-form), which are manifested by the formation of open circular forms (OC-forms), or alternatively, double-strand breaks, which are evident from the formation of linear forms (L-forms). The identification and distribution of different forms were determined by agarose gel electrophoresis. Additionally, the above mentioned reactive species can cleave the DNA into smaller fragments (shown in electrophoreogram as a smear) or even yield complete DNA cleavage.

Reaction without the reducing agent. In the absence of a reducing agent, Fenton's reaction proceeds very slowly. Iron(II) sulphate, used as a reference compound, showed low reactivity with the model circular plasmid molecule. At a molar ratio of $FeSO_4$:1bp (pair of bases in DNA) of 10 : 1 (200 μM concentration), the average DNA cleavage was only 19.1 ± 1.92% (for a detailed report, see ESI Table S4†). Analogous results were obtained for complexes **1** and **3** (see ESI Table S5 and S6†). On the other hand, complexes **2**, **4**, **5**, and **6** cleaved DNA with significantly higher effectiveness at lower concentrations than the reference compound $FeSO_4$ (see ESI Table S7–S10†), suggesting that these complexes either employ stronger interaction with DNA or create more efficient production system in the Fenton's reaction yielding oxidatively damaged polynucleotide chain, especially in the C1′, C4′ and C5′ positions of the deoxyribose residue, leading to subsequent fragmentation.[42,43]

Reaction with the reducing agent. The presence of a reducing agent in high excess in the reaction system strongly increases DNA

Table 7 Spectral shift analysis for complexes **1–6** during DNA titration, showing the maxima of charge-transfer bands at the given ratios of CT-DNA *vs.* complex

	λ_{max} CT-band (unbound form; nm)	Hypochromicity maximum at R^a (%)	Blue(–) or red(+) shift (nm)
1	382	29 (0.71)	–8
2	356; 400	17.1 (0.10)	+2
3	408	n/a	+2
4	394	4.7 (0.53)	0
5	390	3.9 (2.41)	+8
6	422	n/a	0

[a] *R* stands for a ratio of CT-DNA *vs.* complex concentrations (the concentration of DNA is converted to the molar concentrations of its single bases); the *R* values are given in parentheses; n/a = not detected

cleavage efficiency. The increase in efficiency is probably due to the formation of a cyclic production system, in which ascorbic acid reduces Cu(II) to Cu(I) and then copper is re-oxidized by Fenton's reagent, with hydroxyl radical formation. The whole cycle can thus run until complete depletion of the reducing agent or stabilization of the copper oxidation state, *e.g.* by coordination with albumin.[44]

The results of DNA cleavage studies have been found to be in good correlation with *in vitro* antitumour activity of the tested Cu(II) complexes. This may indicate that the interaction with DNA and mainly the ability of copper(II) complexes to act as chemical nucleases are important in the mechanism of their action in biological systems.

Correlation between cytotoxicity and DNA cleavage

In addition to DNA interaction and DNA cleavage studies, we strived to find the correlation between the *in vitro* cytotoxicity and nuclease activity. We found very good correlation between these two properties, which can be expressed in the form of the correlation coefficients, with $R = 0.999$ (for the correlation between the cytotoxicity to the HOS cell line *vs.* the percentage of DNA cleavage at 20 μM in the experiment without the addition of ascorbate, as seen in Fig. 7), $R = 0.986$ (for the correlation between the cytotoxicity to the HOS cell line *vs.* the percentage of DNA cleavage at 20 μM in the experiment with the addition of ascorbate), $R = 0.922$ (for the MCF-7 cell line without the addition of ascorbate), and $R = 0.930$ (for the MCF-7 cell line with the addition of ascorbate as seen in ESI Fig. S14†). Based on these findings, we may conclude that there exists a relationship between the *in vitro* cytotoxicity and nuclease activity of the studied complexes. Moreover, it could serve as an effective tool for the prediction and evaluation of *in vitro* cytotoxicity of newly prepared compounds of similar composition and stereochemistry after the model extension and validation in future.

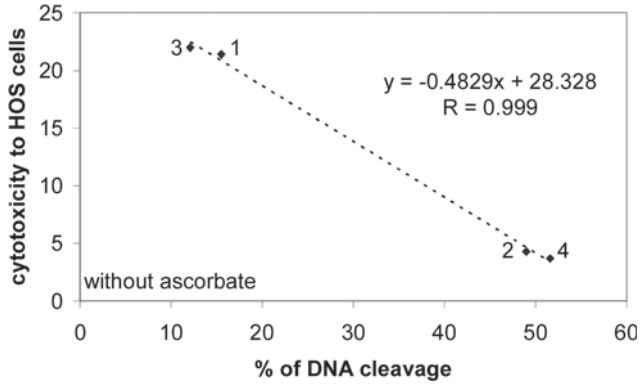

Fig. 7 The correlation between the cytotoxicity to HOS cell line *vs.* the percentage of DNA cleavage at 20 μM in experiment without the addition of ascorbate for complexes **1**–**4**.

Cytological visualization of copper

In order to confirm the ability of complexes **1**–**6** to penetrate living cells, a method called as a rhodanine method routinely used for cytological diagnostic of the Wilson's disease was carried out.[45] This method is based on the formation of brown-red coloured copper(II) complex with 5-(dimethylamino)benzylidenerhodanine. The cells with increased levels of intracellular copper were stained red-brown. The intensity of red-brown colour of cells cultured with complex **2** (see ESI Fig. S15†) compared to the control sample cultured with vehicle (see ESI Fig. S16†), leads to the conclusion that complex **2** penetrates into living cells of THP-1.

Interaction with human serum albumin

ESI-MS analysis of a mixture of complex **2** with HSA was performed in order to determine whether the complexes are able to interact with biomolecules.[46]

Comparison of deconvoluted MS spectra of pure HSA with the mixtures of complex **2** *vs.* HSA in molar ratios 1 : 1 and 10 : 1 revealed that the interaction of complex **2** with the HSA was observed only in the 10 : 1 case. The interaction is probably caused by the ligand exchange of qui for the appropriate binding site at HSA. At these conditions, we identified that the coordination species $Cu(phen)^{2+}$ bind to the protein in a 1 : 1 ratio. The presence of the complex [protein–$Cu(phen)(H_2O)$] was confirmed by the appearance of a deconvoluted peak at 66 123 Da, which represents a 258 Da (see ESI Fig. S17†) difference from the mean deconvoluted mass of intact HSA (65 865 Da) (see ESI Fig. S18†), corresponding to the species of $[Cu(phen)(H_2O)]^{2+}$.

The stability of the complex **2** during the ESI-MS analysis was monitored as well. In each experimental step in which complex **2** was involved, we were able to observe the specific masses characteristic for the intact complex (479.16 corresponding to $(M–NO_3)^+$ and 302.08 corresponding to $Cu(phen)(acetate)^+$) in the range of 80–600 m/z. This observation confirms that even in the presence of a strong chelating agent, complex **2** is stable enough to be able to provide a pharmacologically active coordination species with the ability to bind to the structure of a transport protein such as HSA.

Conclusions

We prepared and fully characterized a series of mixed-ligand Cu(II) complexes with the 2-phenyl-3-hydroxy-4(1*H*)-quinolinonate anion (qui) of the formulas $[Cu(qui)(bpy)]NO_3·1/2H_2O$ (**1**), $[Cu(qui)(phen)]NO_3·H_2O$ (**2**), $[Cu(qui)(ambpy)]NO_3·1/2H_2O$ (**3**), $[Cu(qui)(mphen)]NO_3·H_2O$ (**4**), $[Cu(qui)(nphen)]NO_3·H_2O$ (**5**) or $[Cu(qui)(bphen)]NO_3·H_2O$ (**6**). The X-ray molecular structures of the complexes **2** and **3a** exhibited Cu(II) in the distorted square-planar geometry.

The results of *in vitro* cytotoxicity obtained for complexes **1**–**4** and **6** against the HOS and MCF7 human cancer cell lines are significantly better than those of cisplatin, a commercially used antineoplastic drug, for the same cancer cell lines. Relatively strong intercalating ability of the complexes to DNA showed the possible mechanism of the cytotoxic effect of the prepared Cu(II) complexes against the above-mentioned human cancer cell lines. It can be seen from the obtained results that we not only prepared and characterized novel type of Cu(II) complexes involving the 2-phenyl-3-hydroxy-4(1*H*)-quinolinonate anion but also found that the obtained results regarding anticancer activity are very promising and thus, the biological properties of such systems should be studied in greater details in future. Based on these findings, we may also conclude that there exists a good correlation between the *in vitro* cytotoxicity and nuclease activity, which could

serve (after the model extension and validation) as an effective tool for the prediction of cytotoxicity of newly prepared compounds of similar composition and stereochemistry in future.

Acknowledgements

The authors gratefully thank the Ministry of Education, Youth and Sports of the Czech Republic (MSM6198959218), the Operational Program Research and Development for Innovations - European Regional Development Fund (CZ.1.05/2.1.00/03.0058), the Operational Program Education for Competitiveness - European Social Fund (project CZ.1.07/2.3.00/20.0017) of the Ministry of Education, Youth and Sports of the Czech Republic, and GAČR P207/11/0841 for financial support, Dr Pavel Štarha for performing TG/DTA experiments, Ms. Radka Novotná for measuring infrared and Raman spectra, Ms. Alena Klanicová for mass spectra measurements, Dr Jan Hošek for technical assistance with cytological visualization of intracellular copper, and Dr Peter Baran for useful discussions.

Notes and references

1 E. Wong and C. M. Giandomenico, *Chem. Rev.*, 1999, **99**, 2451.
2 E. R. Jamieson and S. J. Lippard, *Chem. Rev.*, 1999, **99**, 2467.
3 M. J. Burkitt, *Methods Enzymol.*, 1994, **234**, 66.
4 J. Kang, C. Lin, J. Chen and Q. Liu, *Chem.-Biol. Interact.*, 2004, **148**, 115.
5 N. S. Aston, N. Watt, I. E. Morton, M. S. Tanner and G. S. Evans, *Hum. Exp. Toxicol.*, 2000, **19**, 367.
6 C. A. Grillo, M. A. Reigosa, M. Fernández and L. de Melle, *Mutat. Res.*, 2009, **672**, 45.
7 T. Theophanides and J. Anastassopoulou, *Crit. Rev. Oncol. Hematol.*, 2002, **42**, 57.
8 V. S. Narayanan, C. A. Fitch and C. W. Levenson, *J. Nutr.*, 2001, **131**, 1427.
9 F. P. Dwyer, E. Mayhew, E. M. Roe and A. Shulman, *Br. J. Cancer*, 1965, **19**, 195.
10 P. U. Maheswari, M. van der Ster, S. Smulders, S. Barends, G. P. van Wezel, C. Massera, S. Roy, H. den Dulk, P. Gamez and J. Reedijk, *Inorg. Chem.*, 2008, **47**, 3719.
11 S. S. Hindo, M. Frezza, D. Tomco, M. J. Heeg, L. Hryhorczuk, B. R. McGarvey, Q. P. Dou and C. N. Verani, *Eur. J. Med. Chem.*, 2009, **44**, 4353.
12 D. Chen, V. Milacic, M. Frezza and Q. P. Dou, *Curr. Pharm. Des.*, 2009, **15**, 777.
13 S. Tardito and L. Marchio, *Curr. Med. Chem.*, 2009, **16**, 1325.
14 A. De Vizcaya-Ruiz, A. Rivero-Muller, L. Ruiz-Ramirez, G. E. N. Kass, L. R. Kelland, R. M. Orr and M. Dobrota, *Toxicol. in Vitro*, 2000, **14**, 1.
15 C. Mejia and L. Ruiz-Azuara, *Pathol. Oncol. Res.*, 2008, **14**, 467.
16 M. E. Bravo-Gomez, J. C. Garcia-Ramos, I. Garcia-Mora and L. Ruiz-Azuara, *J. Inorg. Biochem.*, 2009, **103**, 299.
17 K. Hoshino, K. Sato, K. Akahane, A. Yoshida, I. Hayakawa, M. Sato, T. Une and Y. Osada, *Antimicrob. Agents Chemother.*, 1991, **35**, 309.
18 M. Suto, J. M. Domagala, G. E. Roland, G. B. Mailloux and M. A. Cohen, *J. Med. Chem.*, 1992, **35**, 4745.
19 S. Radl and S. Dax, *Curr. Med. Chem.*, 1994, **1**, 262.
20 M. Soural, J. Hlaváč, P. Hradil, I. Fryšová, M. Hajdúch, V. Bertolasi and M. Maloň, *Eur. J. Med. Chem.*, 2006, **41**, 467.
21 M. Czaun, G. Speier and L. Parkanyi, *Chem. Commun.*, 2004, **8**, 1004.
22 R. Vrzal, P. Štarha, Z. Dvořák and Z. Trávníček, *J. Inorg. Biochem.*, 2010, **104**, 1130.
23 S. Satyanarayana, J. C. Dabrowiak and J. B. Chaires, *Biochemistry*, 1992, **31**, 9319.
24 Z. D. Xu, H. Liu, S. L. Xiao, M. Yang and X. H. Bu, *J. Inorg. Biochem.*, 2002, **90**, 79.
25 F. A. Allen, *Acta Crystallogr., Sect. B: Struct. Sci.*, 2002, **58**, 380.
26 A. B. P. Lever, *Inorganic Electronic Spectroscopy*, Elsevier, Amsterdam, 1968.
27 A. Barve, A. Kumbhar, M. Bhat, B. Joshi, R. Butcher, U. Sonawane and R. Joshi, *Inorg. Chem.*, 2009, **48**, 9120.
28 S. Stoll and A. Schweiger, *J. Magn. Reson.*, 2006, **178**, 42.
29 B. J. Hathaway, *Copper in Comprehensive Coordination Chemistry: The Synthesis, Reactions, Properties, and Applications of Coordination Compounds. Volume 5: Late Transition Elements*. Edited by Sir Geoffrey Wilkinson (Pergamon Press, Maxwell House, Fairview Park, Elmsford, New York 10523), 1987.
30 R. Boča, *Theoretical foundation of molecular magnetism*; Elsevier: Amsterdam, 1999.
31 D. C. Johnston, R. K. Kremer, M. Troyer, X. Wang, A. Klumper, S. L. Buďko, A. F. Panchula and P. C. Canfield, *Phys. Rev. B*, 2000, **61**, 9558.
32 Z. Trávníček, R. Herchel, J. Mikulík and R. Zbořil, *J. Solid State Chem.*, 2010, **183**, 1046.
33 M. R. Ayani, A. Hassanpour, A. K. Bordbar and V. Mirkhani, *Bull. Korean Chem. Soc.*, 2009, **30**, 1973.
34 B. C. Bales, M. Pitié, B. Meunier and M. M. Greenberg, *J. Am. Chem. Soc.*, 2002, **124**, 9062.
35 B. C. Bales, T. Kodama, Y. N. Weledji, M. Pitié, B. Meunier and M. M. Greenberg, *Nucleic Acids Res.*, 2005, **33**, 5371.
36 J. M. C. Gutteridge, *Free Radical Res.*, 1993, **19**, 141.
37 W. K. Pogozielski and T. D. Thullius, *Chem. Rev.*, 1998, **98**, 1089.
38 M. Pitié and G. Pratviel, *Chem. Rev.*, 2010, **110**, 1018.
39 T. B. Thederahn, M. D. Kuwabara, T. A. Larsen and D. S. Sigman, *J. Am. Chem. Soc.*, 1989, **111**, 4941.
40 M. M. Meijler, O. Zelenko and D. S. Sigman, *J. Am. Chem. Soc.*, 1997, **119**, 1135.
41 O. Zelenko, J. Gallagher, Y. Su and D. S. Sigman, *Inorg. Chem.*, 1998, **37**, 2198.
42 A. Bencini and V. Lippolis, *Coord. Chem. Rev.*, 2010, **254**, 2096.
43 P. C. Dedon, *Chem. Res. Toxicol.*, 2008, **21**, 206.
44 T. Kocha, M. Yamaguchi, H. Ohtaki, T. Fukuda and T. Aoyagi, *Biochim. Biophys. Acta, Protein Struct. Mol. Enzymol.*, 1997, **1337**, 319.
45 K. Okamoto, M. Utamura and G. Mikami, *Trans. Soc. Pathol. Jpn.*, 1938, **22**, 348.
46 J. Talib, J. L. Beck and S. F. Ralph, *JBIC, J. Biol. Inorg. Chem.*, 2006, **11**, 559.

